JOURNAL OF MATERIALS SCIENCE **37** (2002) 663–668

Sintering and piezoelectric properties of $Pb(Ni_{1/3}Sb_{2/3})O_3$-$PbZrO_3$-$PbTiO_3$ ceramics

MOO-CHIN WANG
Department of Mechanical Engineering, National Kaohsiung University of Applied Sciences, 415 Chien-Kung Road, Kaohsiung, 80782, Taiwan

MAO-SUNG HUANG, TZE-SHEONG WONG, NAN-CHUNG WU
Department of Materials Science and Engineering, National Cheng-Kung University, 1 Ta-Hsueh Road, Tainan, 70101, Taiwan

The sintering and piezoelectric properties of $Pb(Ni_{1/3}Sb_{2/3})O_3$-$PbZrO_3$-$PbTiO_3$ ceramics have been investigated. When the powders contain 48 mol% $PbTiO_3$ and less than 10 mol% $Pb(Ni_{1/3}Sb_{2/3})O_3$ followed by calcination at 850°C for 2 h, the calcine only contains the perovskite structure; but if the $Pb(Ni_{1/3}Sb_{2/3})O_3$ content is between 12 mol% and 14 mol%, both tetragonal and rhombohedral phases are obtained. The composition of the morphotropic phase boundary(MPB) in the $Pb(Ni_{1/3}Sb_{2/3})O_3$-$PbZrO_3$-$PbTiO_3$ system is $Pb(Ni_{1/3}Sb_{2/3})O_3 = 12$ mol%, $PbZrO_3 = 40$ mol% and $PbTiO_3 = 48$ mol%. As the composition at the MPB is sintered at 1260°C and 1280°C for 2 h, respectively, the maximum density (7.8 g/cm^3) is obtained. The SEM micrographs indicate that a decrease in porosity with increasing sintering temperature is attained at 1280°C, which is due to a decrease in the number and size of pores. When the sintering temperature is higher than 1280°C, the porosity increases due to PbO evaporation leading to an increase of the number of pore sites and in enlargement of the pore diameter. When the compact composition at MPB is sintered at 1280°C for 2 h, the planar coupling coefficient (K_p) and mechanical quality coefficient (Q_m) tend to approach the maximum (0.488) and minimum values (292.5), respectively. © *2002 Kluwer Academic Publishers*

1. Introduction

Lead zirconate-titanate (PZT) is such an important piezoelectric ceramic that much attention is given to its piezoelectric properties and it is widely used for piezoelectric devices [1–3]. Lead based ferroelectric relaxor materials of the form $Pb(B'B'')O_3$ show unusually high dielectric constants with a broad dielectric maxima [4]. A number of relaxor materials can be fired at relatively low temperatures compared with the barium titanite based system and they are promising condidate materials for capacitor, transducer and micropositioner applications [5–7].

The understanding of certain physical phenomena in piezoelectric ceramic has developed continuously during the last few decades and presently it is possible to discuss in some detail the physics of piezoelectric ceramics [2]. Shirane *et al.* [8, 9] studied lead zirconate-lead titanate solid solution and found a morphotoropic phase transformation. The crystal structure changed from tetragonal to rhombohedral in the vicinity of Zr/Ti = 53/47 corresponding to a composition of the morphotropic phase boundary (MPB) [3]. Jaffe *et al.* [10] found the excellent piezoelectric properties as well for the composition $Pb(Zr_{0.55}Ti_{0.45})O_3$ near the MPB composition where the morphotropic transformation between tetragonal and rhombohedral takes place.

On the other hand, Ouchi *et al.* [11] have pointed out that $Pb(Mg_{1/3}Nb_{2/3})O_3$-$PbZrO_3$-$PbTiO_3$ compositions near the MPB (between tetragonal and pseudocubic or rhombohedral phases) form a solid solution of a perovskite-type structure and have a high dielectric constant and a high planar coupling coefficient. Although they possess a high potential as an electromechanical transducing material, the mechanical Q-factor is too low to permit their use as a resonator in filter circuits [11]. In addition to a high mechanical Q-factor, a high-dielectric constant and a high planar coupling coefficient (K_p) are desirable for transducers in phonograph pickups and in ultransonic vibrations. Many researchers have reported on the $PbTiO_3$-$PbZrO_3$ system with the effect of additive on the piezoelectric properites [12–14].

In recent years, lead-based perovskites such as $Pb(Mg_{1/3}Nb_{2/3})O_3$ have shown a great promise for applications in both capacitors and electrostrictive actuators [15, 16]. However, it is well known, that piezoelectric relaxor materials such as $Pb(Mg_{1/3}Nb_{2/3})O_3$ are difficult to prepare without the coexistence of the pyrochlore phase. In Taiwan piezoelectric materials have a great demand in the market of the device filters, ultrasonic system, etc. Besides, the piezoelectric materials and devices have a longer life cycle. In the present study, Ni and Sb are used to replace Mg and Nb, respectively, in $Pb(Mg_{1/3}Sb_{2/3})O_3$-$PbZrO_3$-$PbTiO_3$ ceramics has a perovskite structure without pyrochlore.

The piezoelectric properties of relaxors are very sensitive to processing variables such as calcination, firing temperature and stoichimetry of the composition. The present work was undertaken to investigate the sintering and piezoelectric properties of the $Pb(Ni_{1/3}Sb_{2/3})O_3$-$PbZrO_3$-$PbTiO_3$ (PNS-PZ-PT for short) ceramics. The objectives of this investigation were to (i) evaluate the stability of the perovskite structure, (ii) demonstrate the effect of sintering temperature on the density, (iii) assess the effect of composition and sintered temperature on the planar coupling coefficient (K_p) and mechanical quality coefficient (Q_m) and (iv) elucidate the microstructure change of PNS-PZ-PT ceramics during sintering.

2. Experimental procedure

2.1. Sample preparation

Several compositions in the xPNS-(52-x)PZ-48PT($2 \leqq x \leqq 14$) and 12PNS-($88-y$)PZ-yPT($44 \leqq y \leqq 52$) systems were prepared by a mixed oxide method. The raw materials of PbO (purity >98%, supplied by Santoku Chemical Co. Ltd., Japan), TiO_2 (Purity >99%, supplied by MERCK, Germany) ZrO_2 (Purity >99.9%, supplied by Showa Chemicals Inc., Japan), NiO (purity >99.9%, supplied, by FERAK, Germany) and Sb_2O_3 (purity >99.9%, supplied by FERAK, Germany) were weighted and mixed. Each mixture of the starting powders was milled and mixed in a centrifugal mill, as well as wet-homogenized with distilled water for 8 h using high purity Al_2O_3 balls (SSA-S standard 99.5%, diameter 1.0 cm). The obtained powder was dried in an oven, subsequently mixed and dried in a covered alumina crucible (SSA-S standard) and lastly calcined at 850°C for 8 h with a heating rate of 350°C/h.

The calcined powders were reground using wet ball-milling for 15 min, then dried and sifted. The fine powders were mechanically blended with 1 wt% PVA binder in a high-shear mill for 2 h and sieved after granulation. The powder mixture after granulation (−80& + 120 mesh) was isostatically pressed at 245 MPa into a pellet of 1.50 mm in height and 12.0 mm in diameter.

Finally, the pellets were put in a lump of coarse grained powders of the same composition in a sealed alumina crucible and fired between 1200°C and 1320°C for 2 h with a heating rate of 4°C/min [17]. The sinter was lapped to a thickness of 1.0 mm. An electrode was fitted by painting the body with silver paste and firing at 780°C for 20 min.

2.2. Analysis

After sintering, the bulk density of all samples was measured by using an Archimedes method using Equation 1.

$$\text{Bulk density} = \frac{D}{W - S}(\text{g/cm}^3) \qquad (1)$$

where D is weight of dried sample, S is weight of sample in water, and W is weight of wet sample.

The phase structure was established by X-ray diffraction (XRD) using Cu Kα radiation and Ni filter, operated at 30 kV, 200 mA, and at a scanning rate of 4°/min (Model Rad II A, Rigaku Co., Tokyo, Japan).

Preceding the piezoelectric measurements, the pellets were poled in a silicone oil at 100°C by applying a static field of 3.5 kV/min for 1 h, and pellets were field-cooled to room temperature in 30 min. Twenty-four hours after poling, the planar coupling coefficient (K_p) [18] and mechanical quality coefficient (Q_m) [19] were computed from the following relation, respectively.

$$K_p = [2.51(f_a - f_r)/f_r]^{1/2} \qquad (2)$$

and

$$Q_m = f_a^2 / 2\pi R_r C f_r \left(f_a^2 - f_r^2\right) \qquad (3)$$

where f_a is antiresonant frequency (cycle/sec), f_r is resonant frequency (cycles/sec), R_r is resonant resistance (ohms) and C is capacity (farads).

The fracture surface of the sintered specimens was examined by a scanning electron microscope (SEM, JEOL 840, Tokyo, Japan).

3. Results and discussion

3.1. Effect of composition on the phase stability

Fig. 1 shows the typical X-ray diffraction (XRD) patterns of the xPNS-(52-x)PZ-48PT ($2 \leqq X \leqq 14$) piezoelectric powders calcined at 850°C for 2 h after ball mixing for 8 h. As the PNS content is lower than 10 mol%, the powders only contain the peroviskite structure. However, the specimens containing from 12 mol% to 14 mol% PNS, show in all cases both phases F_T and F_R, as shown by splitting of the (h00)- and (201)-type reflections in duplets of the $(200)_R$, $(002)_T$, $(112)_R$, and $(211)_T$ peaks. The reflection indexed with T is assigned to the tetragonal piezoelectric phase F_T, whereas that indexed with R to the rhombohedral piezoelectric phase F_R. This phenomenon is caused by increasing PNS content, leading to decreases in the Zr/Ti ratio which affects the phase transition of the PNS-PZ-PT piezoelectric powders.

As the PNS contents is fixed at 12 mol%, the effect of the PT content on the typical mixing for 8 h is shown in Fig. 2. It indicates that as long as the PT content lies between 48 mol% and 44 mol%, the $(200)_R$, $(201)_R$ and $(112)_R$, peaks splits into $(200)_R$ and $(002)_T$, $(201)_R$ and $(102)_T$, $(112)_R$ and $(211)_T$, respectively, illustrating the phase transformation from F_T to F_R. The composition of PNS = 12 mol%, PZ = 40 mol% and PT = 48 mol% is accompanied with the coexistence of the F_T and F_R phases and is called the composition of the morphotropic phase boundary (MPB). The coexistence of both piezoelectric phases at the MPB composition

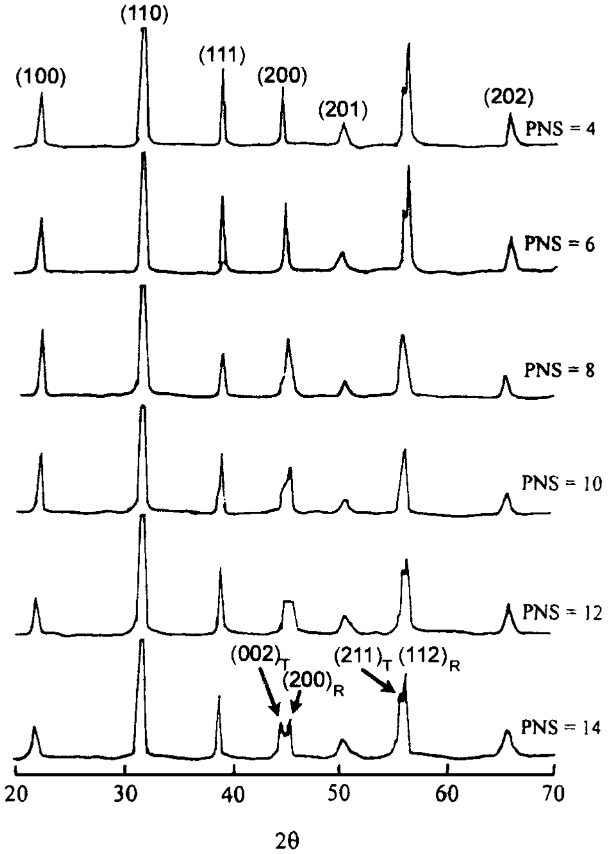

Figure 1 XRD patterns of xPNS-(52−x) PZ-48PT piezoelectric powders calcined at 850°C for 2 h, showing the pervoskite structure ($x < 12$) and tetragonal to rhombohedral transformation at $12 \leq x \leq 14$.

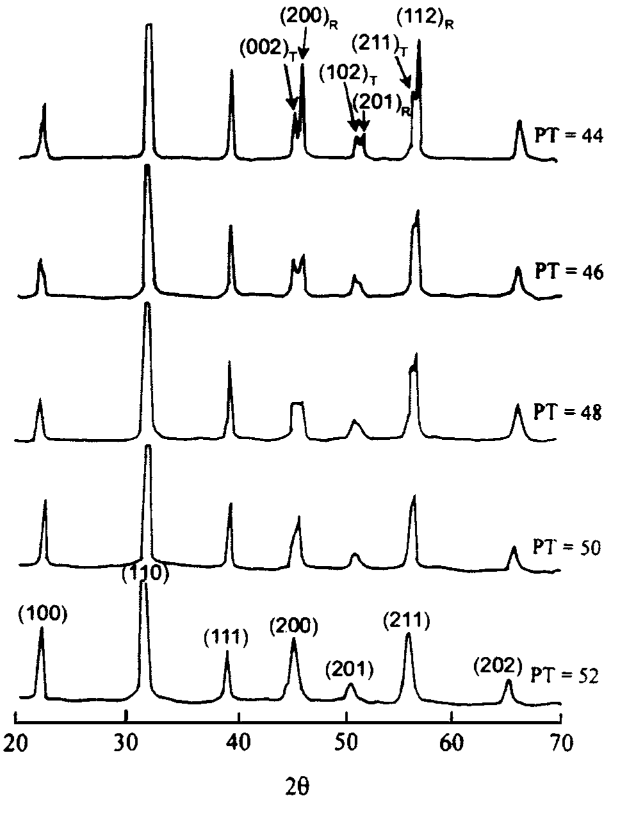

Figure 2 Effect of PT content on the typical XRD patterns of the 12 PNS-(88−x)PZ-xPT($44 \leq x \leq 52$) piezoelectric powders calcined at 850°C for 2 h, showing the tetragonal to rhombohedral transformation.

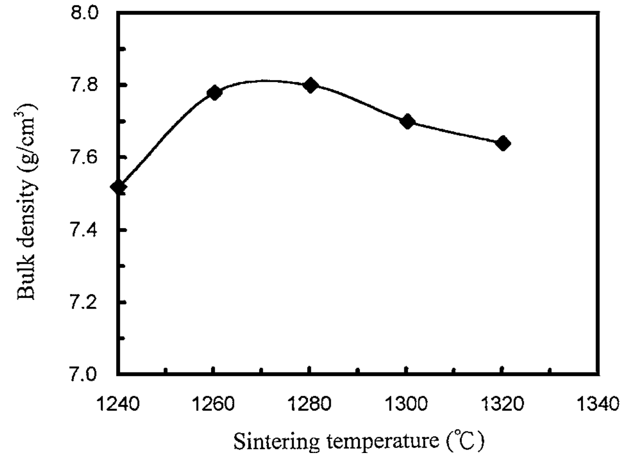

Figure 3 The bulk density of the base composition 12PNS-40PZ-48PT sintered at various temperatures for 2 h.

had been previously demonstrated by XRD in different piezoelectric ceramic systems by splitting of the (200) diffraction peak only [20, 21], the two peaks (200) and (222) [22] or splitting of the (h00)-and (h01)-peaks in the triplets of the $(00h)_T$, $(h00)_R$ and $(h00)_T$, $(h01)_T$, $(h01)_R$ and $(10h)_T$, respectively [23].

3.2. Bulk density and microstructure of the sintered specimens

The effect of sintering temperature on the sintered compact density of the base composition contains 48 mol% PT and 12 mol% PNS, and sintered at various temperatures for 2 h is shown in Fig. 3. The maximum density (7.8 g/cm^3) is obtained when sintered at 1260°C and 1280°C. When the sintering temperature is lower than 1260°C or higher than 1280°C, the sintered compact density is lower. In the densification of the PZT-type ceramics, the sintering temperature is known to play an important role, because the process involves a decrease in the number and size of pores accompanied by an increased densification of grains [24].

The optimum sintering temperature is taken as that where the evaporation and the PbO vapor recondensation equilibrium is attained for PbO vapor as shown below [25]

$$PbO_{(solid)} \Leftrightarrow PbO_{(vapor)} \Leftrightarrow Pb_{(vapor)} + 1/2O_2 \qquad (4)$$

The density decreases when the sintering temperature is higher than 1280°C, due to an increase in porosity (see Fig. 4d and e). This is attributed to a greater rate of evaporation of PbO as compared to that of recondensation.

The size distribution of pores can be obtained qualitatively by means of scanning electron microscope(SEM) examination of the fractured specimens. The SEM micrographs of the specimens containing 48 mol% PT and 12 mol% PNS, and sintered at various temperatures for 2 h are shown in Fig. 4. This indicates a decreases in porosity with increasing sintering temperature up to 1280°C due to a decrease in the number and size of the pores (Fig. 4a–c). After the minimum porosity a further increase in sintering temperature leads to an increase in

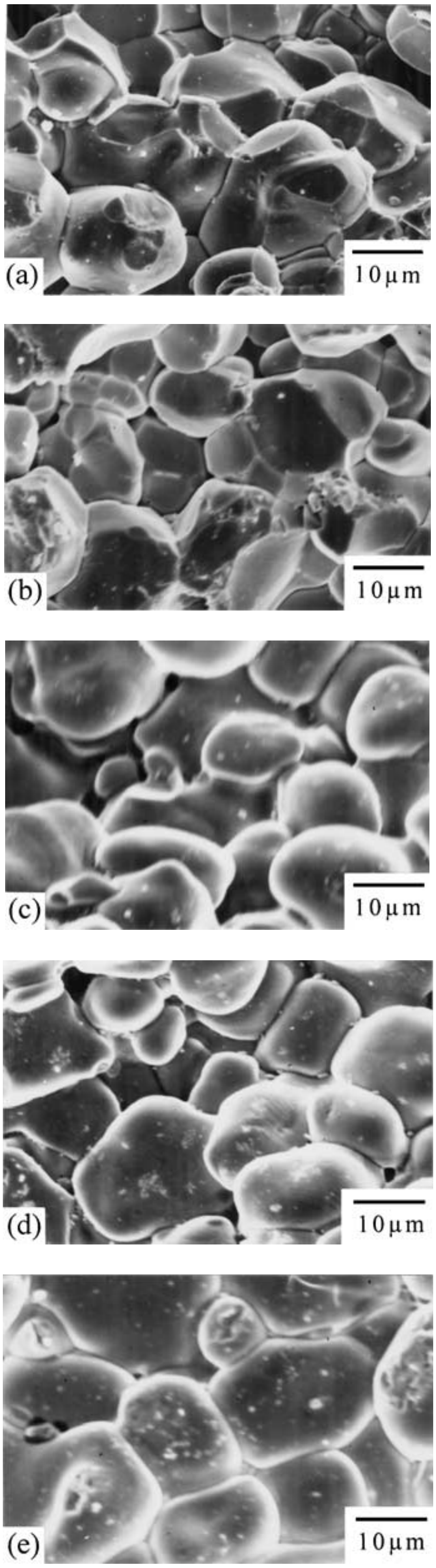

Figure 4 The SEM micrographs of the 12PNS-40PZ-48PT powders sinterded at various temperatures for 2 h: (a) 1240°C, (b) 1260°C, (c) 1280°C, (d) 1300°C and (e) 1320°C.

porosity because of increased PbO evaporation which results in an increased pore size and enlarged pore diameter (Fig. 4d and e).

Fig. 4 also indicates that the grains of the samples sintered at 1240°C and 1260°C for 2 h, respectively, maintain their initial morphology, and these result correspond with some previous data [26] in which octahedral grains are reported to occur at 1250°C. Nevertheless, the grain size increase is higher than in the present study. For the sintering temperature lower than 1260°C, the average grain diameter is practically the same (10–12 μm), but for the higher sintering temperature (1280°C to 1320°C) this value (14–21 μm) is greater than for at 1260°C. On the other hand, when the sintering temperature is higher than 1260°C, the grains have the different morphology. The different sizes as well as the morphological modification, of grains are noticable in these samples.

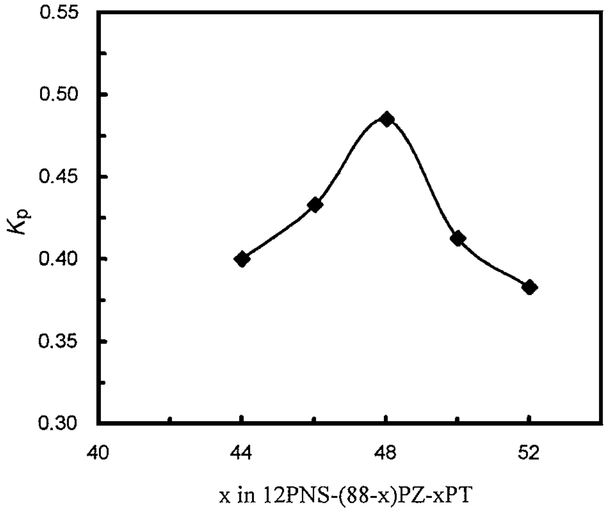

Figure 5 The relation between K_p and x in 12PNS-(88-x)PZ-xPT samples sintered at 1280°C for 2 h.

3.3. K_p and Q_m values of the sintered samples

When the PNS content is fixed at 12 mol% and sintered at 1280°C for 2 h, the K_p value increases from 0.40 to 0.48 with the PT content increasing from 44 mol% to 48 mol%. Conversely, the K_p value decreases from 0.48 to 0.38 as the PT content increases from 48 mol% to 52 mol%. From Figs 2 and 5, it is evident that the composition in MPB yields the highest K_p value.

With the PT content fixed at 48 mol%, the relation of the K_p and Q_m with the PNS content is shown in Fig. 6. It represents the composition of MPB that yields the highest K_p (0.488) and the lowest Q_m (292.5). This result is caused by the coexistence of the F_R and F_T phases at the MPB. Isupor [2] has pointed out that the spontaneous polarization of the F_T phase can be oriented in any one of six crystallographic directions and the F_R phase in any one of eight crystallographic directions. At the MPB, the material can be both tetragonal and rhombohedral, and the spontaneous polarization can be oriented along any one of these fourteen directions.

Fig. 6 also suggests that the K_p and Q_m values decrease gradually with the PNS content varying from 2 mol% to 12 mol% when the PT content is fixed at 48 mol%. On the other hand, the K_p value decreases markedly and the Q_m value increases gradually with the PNS content varying from 12 mol% to 14 mol%. According to Figs 1 and 5, when the PT content is fixed

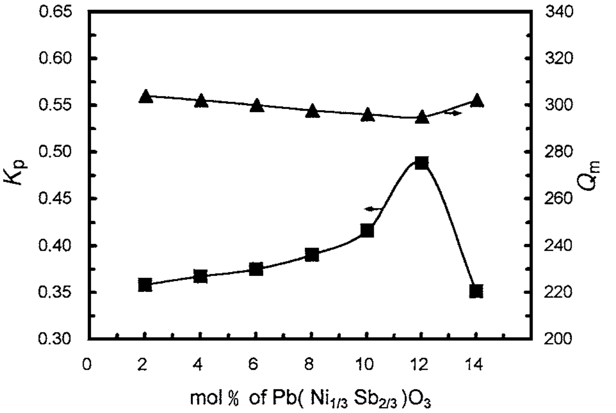

Figure 6 The relationship of K_p and Q_m values with the xPNS-(52-x)PZ-48PT ($2 \leq x \leq 14$) samples sintered at 1280°C for 2 h.

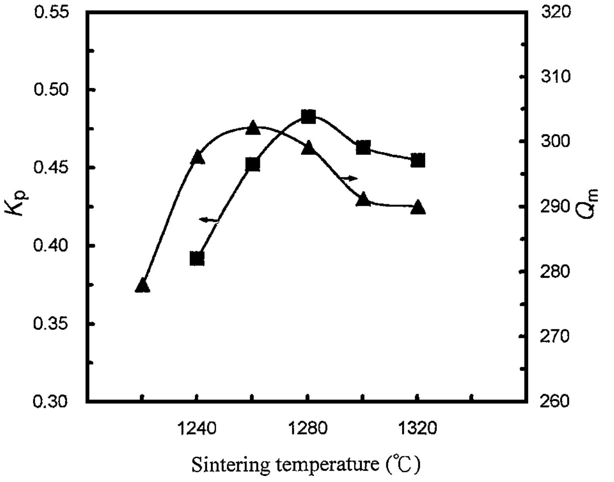

Figure 7 The relationship of K_p and Q_m values with the 12PNS-40PZ-48PT samples sintered at various temperatures for 2 h.

at 48 mol%, an increase in the PNS content decreases the tetragonality of the base composition. Therefore, it is expected that the boundary between the tetragonal and rhombohedral shifts toward the rhobohedral side when the PNS is increased from 4 mol% to 12 mol%.

When the PT and PNS contents are fixed at 48 mol% and 12 mol%, respectively, and sintered at various temperatures for 2 h, the relation of sintering temperature with K_p and Q_m values is shown in Fig. 7. It indicates that when sintered at 1280°C for 2 h, the K_p value approaches the maximum value. When the sintering temperature is lower than 1260°C, the sintered body had the fine grains with poor densification and hence has the lower K_p value. Conversely, when the sintered temperature is higher than 1280°C, the volatility of PbO induces the vacancies in Pb-sites leading to the lower K_p and Q_m values.

Fig. 7 also shows that if sintered at 1260°C for 2 h, the maximum Q_m value is obtained. When the specimens are sintered at 1260°C for 2 h, the fine grain size and good densification have been attained, however, if the sintering temperature is lower than 1240°C or greater than 1280°C, the Q_m value decreases. This result is caused presumably by increased porosity. On the other hand, Mabud [26] has pointed out that a decrease in the width of the coexistence range is associated with sintering temperature and firing time. The compositional fluctuation can lead to the formation of a very small region rich in either lead titanate (tetragonal structure) or lead zirconate (rhombohedral structure) as a function of microscopic concentration and temperature gradient [23]. An increase in sintering temperature enhances the diffusion effect within these regions and leads to a relative homogenization of the local composition.

Figs 4 and 7, indicate an increase in the K_p value accompanied with increased porosity. Generally, a piezoelectric ceramic material is a complete system composed of crystallites, grain boundaries and pores. It is very important to make clear the effect of each microstructural parameter apart from the other parameters. However, this is not so easy because the parameters are coupled to each other [3]. Pores in a piezoelectric material affect the permittivity through the followoing process: the first one is the decreasing of polarization per unit volume and the other is the increasing of the depolarizing field [3].

Figs 4 and 7 also depict that the Q_m value decreases with increasing pore volume. This result is caused by the domain wall motion contribution. In particular, the polling process takes place owing to the domain wall motion [27]. The mechanical quality factor depends on the domain wall hysteresis loss [28]. Piezoelectric domain wall motion is found to be prohibited by the internal bias fields. This results in poling difficulty and a high mechanical quality for the strong internal bias field samples. The internal bias field prohibits the domain wall motion under a small electric signal used for the Q_m-measurement even at room temperature. This is probably the cause of the high Q_m value [27].

4. Conclusions

The sintering and piezoelectric properties of the $Pb(Ni_{1/3}Sb_{2/3})O_3$-$PbZrO_3$-$PbTiO_3$ system has been studied. The results in the present investigation are summarized as follows:

1. When the PT content is fixed at 48 mol%, the xPNS-(52-x)PZ-48PT($2 \leqq x \leqq 14$) powders calcined at 850°C for 2 h, with the PNS content lower than 10 mol%, only contain the pervoskite structure. As the PNS content increases from 12 mol% to 14 mol% the coexistence of both tetragonal and rhombohedral phases is obtained.
2. The composition of PNS = 12 mol%, PZ = 40 mol% and PT = 48 mol% shows the coexistence of the tetragonal and rhombohedral phases and hence is called a MPB composition. Its maximum density (7.8 g/cm^3) is obtained when sintered at 1260°C and 1280°C for 2 h. When the sintering temperature is lower than 1260°C or higher than 1280°C, the sintered density is lower than 7.8 g/cm^3.
3. When the above composition is sintered at 1280°C for 2 h, the K_p and Q_m values attain the maximum (0.488) and minimum value(292.5), respectively.

Acknowledgement

This work was supported by National Science Council, Taiwan, the Republic of China under Contract

No.NSC78-0404-E006-22 for which the authors are very grateful. Experimental aids and suggestion from Prof. M. P. Hung, Prof. M. H. Hon, Mr. S. Y. Yau. and Mr. J. M. Chen are very much appreciated.

References

1. J. J. DIH and R. M. FULRATH, *J. Amer. Ceram. Soc.* **61** (1978) 448.
2. V. A. ISUPOV, *Ferroelectrics* **46** (1983) 217.
3. K. OKAZAKI, *ibid.* **41** (1982) 77.
4. A. VIERHEILING, A. SAFARI and A. HALLIYAL, in "Ceram. Trans," Vol. 8, edited by H. C. Ling and M. F. Yan (American Ceramic Society, Westerville, OH, 1989) p. 75.
5. T. R. SHROUT and A. HALLIYAL, *Am. Ceram. Soc. Bull.* **66** (1987) 704.
6. K. UCHINO, S. NOMURA, L. E. CROSS, S. J. JANG and R. E. NEWNHAM, *J. Appl. Phys.* **51** (1980) 1142.
7. T. R. SHROUT, S. L. SWARTZ and M. J. HAUN, *Am. Ceram. Soc. Bull.* **63** (1984) 808.
8. G. SHIRANE and A. TAKEDA, *J. Phys. Soc. Jpn.* **7** (1952) 5.
9. G. SHIRANE, K. SUZUKI and A. TAKEDA, *ibid.* **7** (1952) 12.
10. B. JAFFE, S. R. ROTH and S. MARZULLO, *J. Appl. Phys.* **25** (1954) 809.
11. H. OUCHI, K. NAGANO and S. HAYAKAWA, *J. Amer. Ceram. Soc.* **49** (1966) 577.
12. F. KULCSAR *ibid.* **42** (1959) 343.
13. M. MARUTAKE, Jpn. Patent. 16,673 (1961).
14. F. KULCSUR, U. S. Patent. 3,006,857 (1961).
15. T. R. SHROUT and A. HALLIYAL, *Am. Ceram. Soc. Bull.* **66** (1987) 704.
16. K. UCHINO, *ibid.* **65** (1986) 647.
17. C. E. HALL and J. B. BLUM, *Ferroelectrics* **37** (1981) 643.
18. W. P. MASON and H. JAFFE, *Proc. IRE.* **42** (1954) 921.
19. D. A. BERLINCOURT, C. CMOLIK and H. JAFFE, *ibid.* **48** (1960) 220.
20. P. ARI-GUR and L. BENQUIGUI, *J. Phys. D.* **8** (1975) 1856.
21. L. HANH, K. UCHINO and S. NOMURA, *Jpn. J. Appl. Phys.* **17** (1978) 637.
22. M. V. TURIK, M. F. KUPRIANOV, E. H. SIDORENKO and S. M. ZAITSEV, *Sov. Phys. Tech. Phys.* (Engl. Transl.) **25** (1980) 1251.
23. P. GR. LUCUTA, FL. CONSTANINESCU and D. BARB, *J. Amer. Ceram. Soc.* **68** (1985) 533.
24. B. JAFFE, W. R. COOK and H. JAFFE, "Piezoelectric Ceramics," (Academic Press, London, 1971) p. 135.
25. F. W. NEILSON, *Bull. Am. Phys. Soc.* **2** (1957) 302.
26. S. A. MABUD, *J. Appl. Crystallogr.* **13** (1980) 211.
27. S. TAKAHASHI, *Ferroelectrics* **41** (1982) 143.
28. B. LEWIS, *Proc. Phys. Soc.* **73** (1970) 17.

Received 20 April
and accepted 1 October 2001